Supporting Information

Robust symmetrical electrode with layered perovskite structure for direct hydrocarbon solid oxide fuel cells: $PrBa_{0.8}Ca_{0.2}Mn_2O_{5+\delta}$

Sihyuk Choi,[a,c] Sivaprakash Sengodan,[a] Seonhye Park,[a] Young-Wan Ju,[a] Junyoung Kim,[a] Junji Hyodo,[b] Hu Young Jeong,[c] Tatsumi Ishihara,[b] Jeeyoung Shin*[d] and Guntae Kim*[a]

[a] *Department of Energy Engineering, Ulsan National Institute of Science and Technology (UNIST), Ulsan, 689–798, Korea*

[b] *International Institute for Carbon Neutral Energy Research, Kyushu University, Fukuoka 819-0395, Japan*

[c] *UNIST Central Research Facilities and School of Mechanical and Advanced Materials Engineering, UNIST, Ulsan, 689–798, Korea*

[d] *Department of Mechanical Engineering, Dong-Eui University, Busan 614-714, Korea*

[e] *Materials Science and Engineering, Northwestern University, Evanston, IL, USA*

Supporting Figures

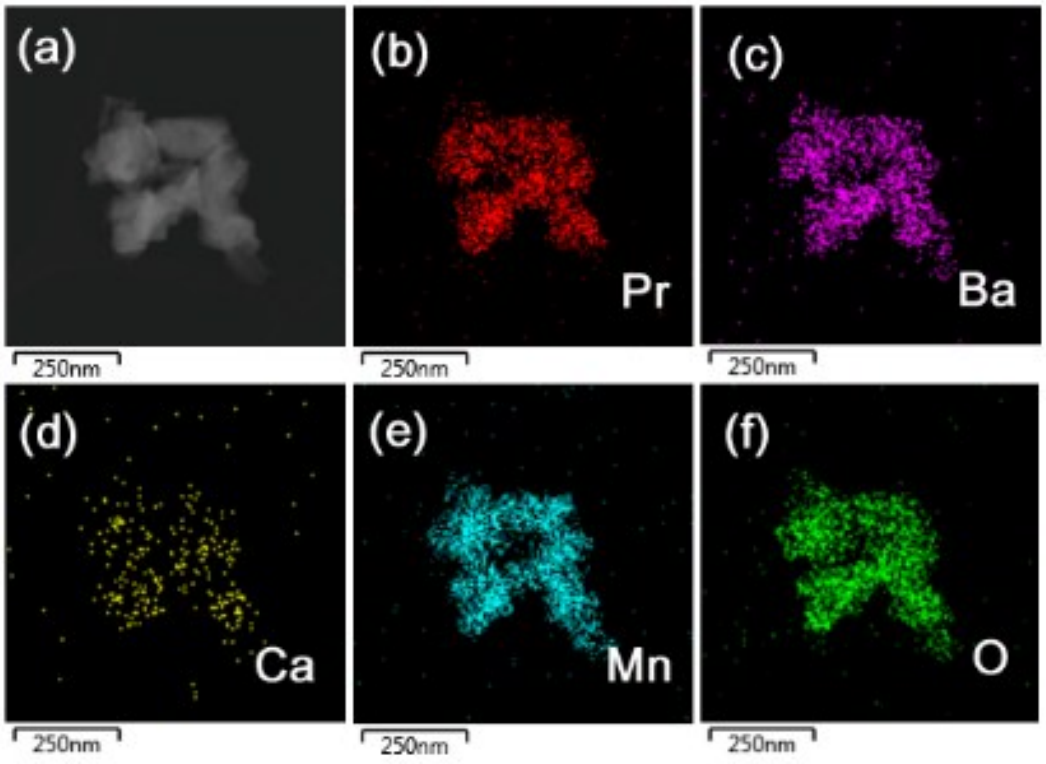

Figure S1. Energy dispersive spectroscopy (EDS) elemental mapping of the layered PBCMO particle. (a) Scanning TEM (STEM) high-angle annular dark-field (HAADF) image. (c-f) Elemental mapping of Pr, Ba, Ca, Mn, and O, respectively.

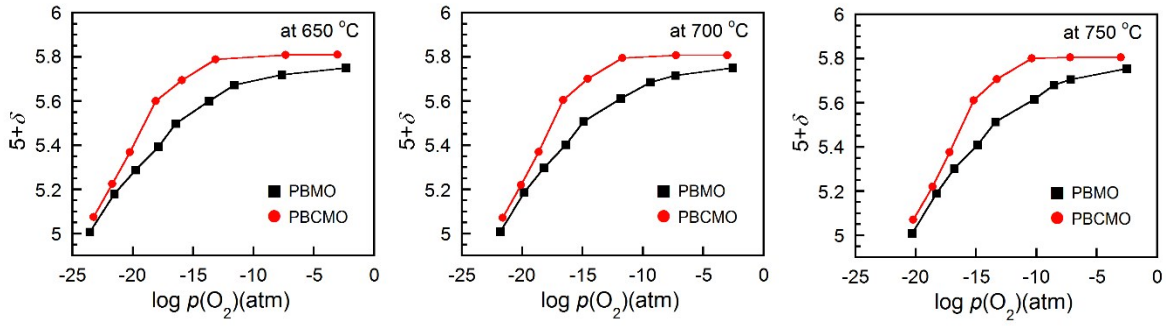

Figure S2. oxygen non-stoichiometry of PBMO and PBCMO at 650, 700, and 750 °C as function of oxygen partial pressure.

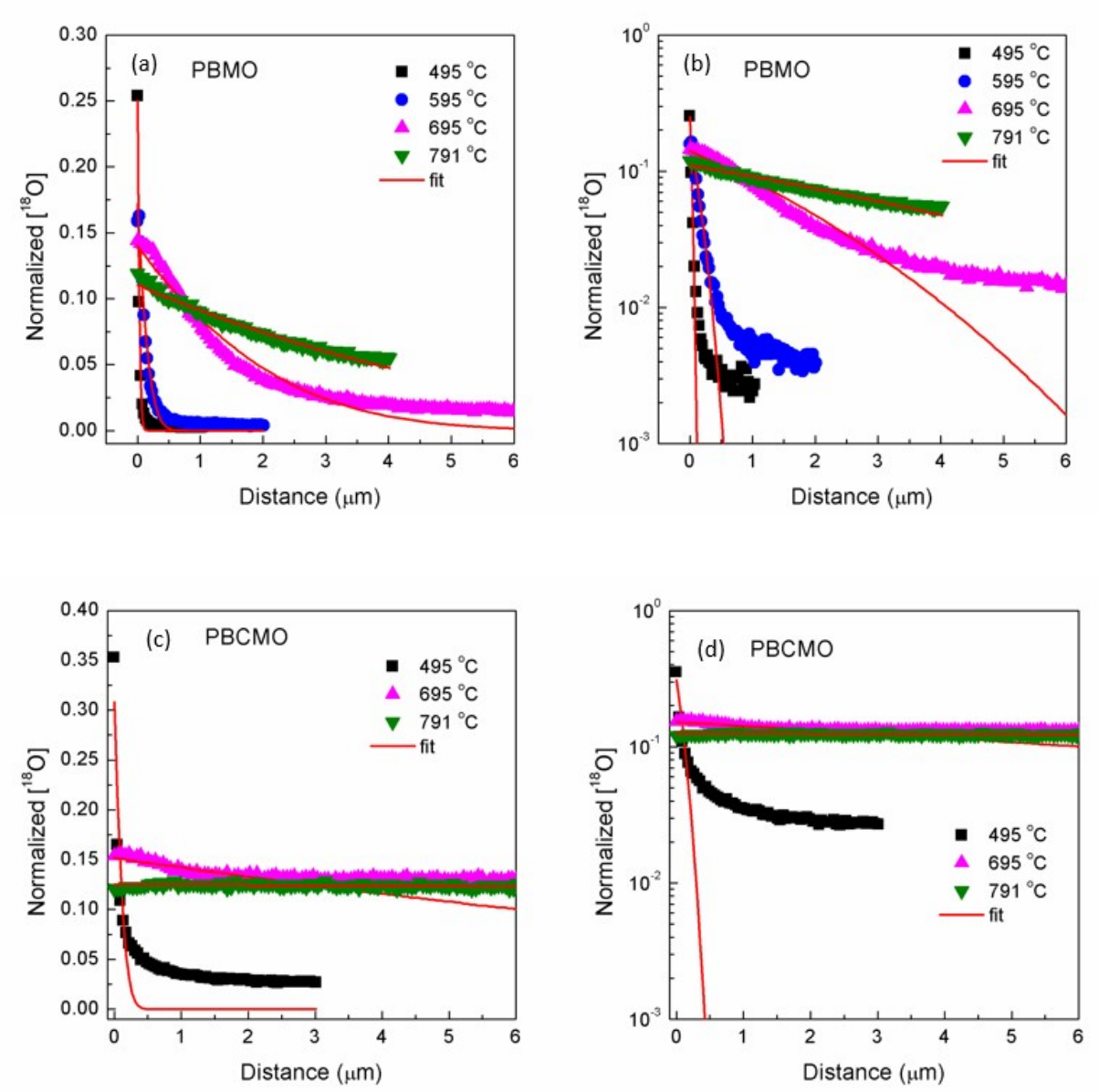

Figure S3. Diffusion profiles of isotope oxygen in PBMO with (a) linear scale and (b) logarithmic scale. Diffusion profiles of isotope oxygen in PBCMO with (c) linear scale and (d) logarithmic scale.

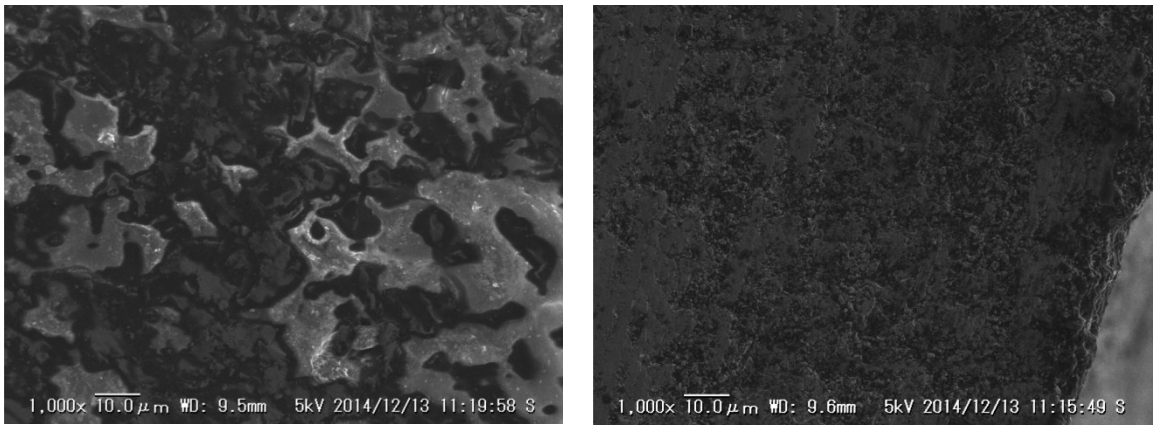

Figure S4. Cross-sectional SEM image of layered PBMO (left) and PBCMO (right) after the oxygen exchange.

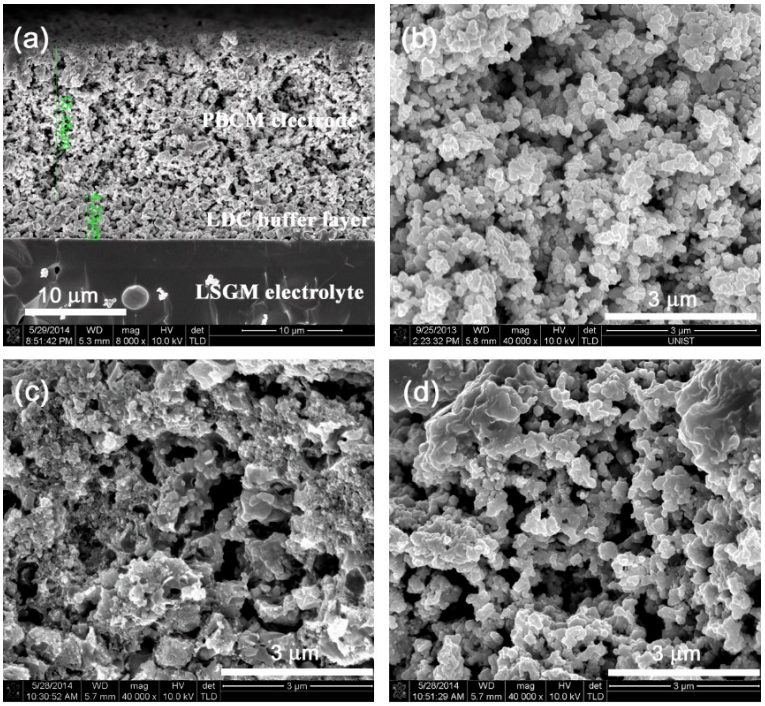

Figure S5. SEM images of (a) cross-section of the single cell, (b) $Pr_{0.5}Ba_{0.4}Ca_{0.1}MnO_3$ electrode after calcination in air at 950 ^oC, (c) 15 wt% of Co-Fe catalyst infiltrated in $Pr_{0.5}Ba_{0.4}Ca_{0.1}MnO_3$ after calcination in air at 450 ^oC, and (d) layered PBCMO electrode with Co-Fe catalyst after annealed in humidified H_2 at 800 ^oC. For cross-sectional single cell, layered PBCMO electrode reveals homogeneously distributed particles and relatively small grain size with good connectivity between grains as well as reasonable porosity, which ensures effective gas diffusion. The LSGM electrolyte appears to be quite dense and strongly adheres with porous LDC buffer layer. It is clear that the microstructures of the single cell display good intimate contact between all interfaces between components. After the infiltration of Co-Fe catalyst and calcination at 450 ^oC, the very fine Co-Fe particles are uniformly distributed onto the PBCMO electrode. And, through the annealing process at 850 ^oC in H_2, thin film of Co-Fe alloy is well covered on the surface of PBCMO electrode.

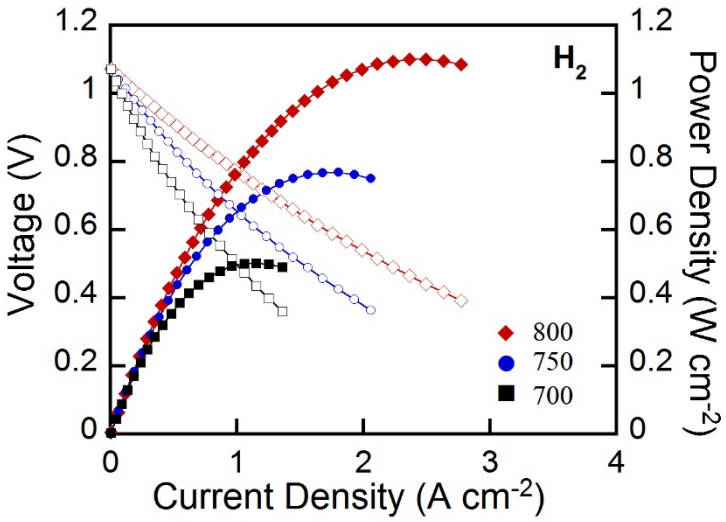

Figure S6. *I-V* curves and the corresponding power densities of layered PBCMO symmetrical cell in humidified H_2.

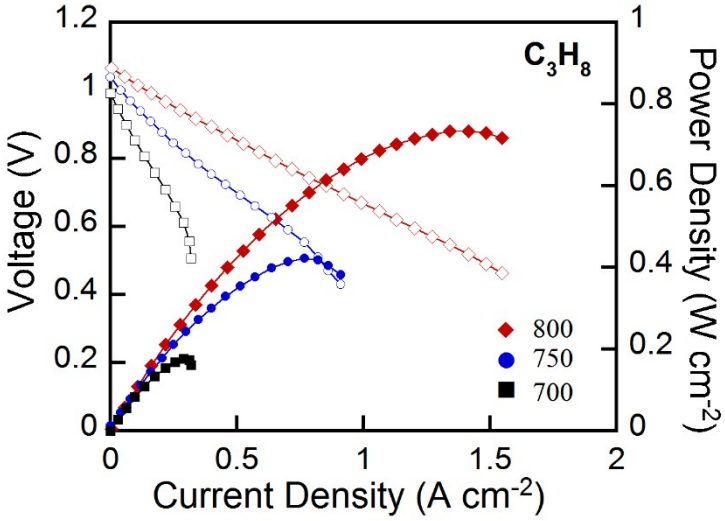

Figure S7. *I-V* curves and the corresponding power densities of layered PBCMO symmetrical cell humidified in C_3H_8.

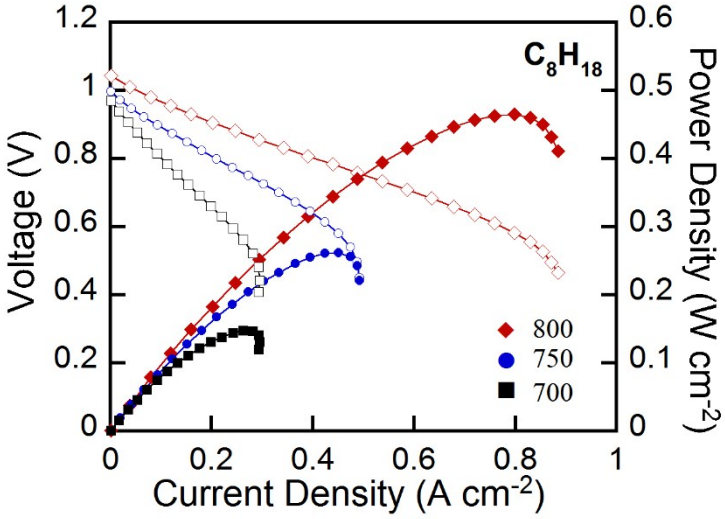

Figure S8. *I-V* curves and the corresponding power densities of layered PBCMO symmetrical cell humidified in C_8H_{18}.

Table. S1. Experimental conditions for isotope oxygen exchange and the detail of obtained oxygen tracer diffusivity (D*), oxygen surface exchange coefficient (k*) and diffusion length ($L_D=2\sqrt{Dt}$).

Sample	Exchange temperature (^oC)	Exchange time (sec)	D* ($cm^2\ s^{-1}$)	k* ($cm\ s^{-1}$)	L_D ($=2\sqrt{Dt}$, cm)
PBMO	491	1200	5.0×10^{-15}	4.6×10^{-10}	4.9×10^{-6}
PBMO	595	1800	9.8×10^{-14}	1.1×10^{-9}	2.7×10^{-5}
PBMO	695	2400	2.2×10^{-11}	1.5×10^{-8}	4.6×10^{-4}
PBMO	791	1800	1.9×10^{-10}	4.2×10^{-8}	1.2×10^{-3}
PBCMO	491	1200	6.9×10^{-14}	2.3×10^{-9}	1.8×10^{-5}
PBCMO	695	1800	1.0×10^{-9}	1.1×10^{-7}	2.7×10^{-3}
PBCMO	791	1800	1.0×10^{-6}	3.6×10^{-6}	8.5×10^{-2}